Variational calculations for $\bar{K}$–few-nucleon systems

S. Wycech*
Andrzej Sołtan Institute for Nuclear Studies, 00-681 Warsaw, Hoza 69, Poland

A. M. Green†
Helsinki Institute of Physics, P. O. Box 64, FIN-00014, Finland

(Received 4 September 2008; revised manuscript received 3 November 2008; published 14 January 2009)

Deeply bound $\bar{K}NN$, $\bar{K}NNN$, and $\bar{K}NNNN$ states are discussed. The effective force exerted by the $\bar{K}$ meson on the nucleons is calculated with static nucleons. Next the binding energies are obtained by solving the Schrödinger equation or by variational calculations. The dominant attraction comes from the S-wave $\Lambda(1405)$ and an additional contribution is due to $\Sigma(1385)$. The latter state is formed at the nuclear peripheries and absorbs a sizable piece of the binding energy. It also generates new branches of quasibound states. The lowest binding energies based on a phenomenological $\bar{K}N$ input fall into the 40- to 80-MeV range for $\bar{K}NN$, 90–150 MeV for $\bar{K}NNN$, and 120–220 MeV for $\bar{K}\alpha$ systems. The uncertainties are due to unknown $\bar{K}N$ interactions in the distant subthreshold energy region.

DOI: 10.1103/PhysRevC.79.014001 PACS number(s): 13.75.Jz, 21.45.−v, 25.10.+s, 25.80.−e

I. INTRODUCTION

In this article a quantitative understanding of antikaon-few-nucleon quasibound states is attempted. In recent years, the existence of such states has been vividly discussed. It was initiated by the KEK finding of peaks in the nucleon spectra of K^- absorption in ^{4}He [1,2]. Additional evidence was given by the FINUDA measurement of the invariant mass distribution of the Λp produced in K^-absorption by light nuclei [3]. The existence of such bound states have been expected as the kaon-nucleon and the kaon-nucleus interactions have been known to be strongly attractive [4]. This is now firmly confirmed on the basis of kaonic atom data [5]. However, the KEK and FINUDA experiments indicate unexpectedly strong bindings of the order of 100, 150 MeV in the lightest $\bar{K}NN$, $\bar{K}NNN$ systems. These experiments require further confirmation. Also, the interpretation of the observed peaks has been disputed in Refs. [6,7], whereas the initial interpretation is defended in Ref. [8].

Calculations indicate that such states are expected, albeit these might be very broad and difficult to detect. The first calculations performed by Akaishi and Yamazaki in Ref. [9] were followed by several subsequent publications. These calculations exploited essentially the S-wave resonant attraction related to the $\Lambda(1405)$ state. With an optical model type of approach it was shown that the $\bar{K}$-meson optical potential at the center of small nuclei may be as strong as 500 MeV, generating very strong binding of the meson and a strong contraction of the few-nucleon systems. However, to reproduce the KEK data, these calculations involved some relaxation of the NN repulsion at short distances that would allow the existence of strongly bound and very dense systems. These calculations raise the important question on how to implement a realistic short-range NN repulsion in the kaonic systems.

Another open question is related to the strength and range of $\bar{K}N$ interactions. Any mathematical description of few-body systems requires knowledge of NN and $\bar{K}N$ off-shell scattering amplitudes. Those related to NN interactions are controlled fairly well in terms of modern NN potentials. For a bound $\bar{K}$ meson the amplitudes needed involve the subthreshold energy region

$$f_{KN} = f_{KN}(-E_B - E_{\text{recoil}}), \tag{1}$$

where E_B is the $\bar{K}N$ separation energy and E_{recoil} the recoil energy of the $\bar{K}N$ pair relative to the rest of the system. If the separation energy is as large as 100 MeV, meson momenta become $\approx$250 MeV/c and E_{recoil} may be as large as 40 MeV. The energies of interest for $(-E_B - E_{\text{recoil}})$ are then located well below the $\Lambda(1405)$ state. The amplitudes there are strongly attractive and so when used in a standard optical potential approach may support very strong bindings. One problem that arises at this stage is of a technical character. As these amplitudes are energy dependent, it is hard to account for that in the optical model approach. There exists another, more serious, problem that is common to all approaches. As the energies involved are far away from the physical region tested in $\bar{K}N$ scattering, the uncertainties in the $\bar{K}N$ scattering amplitudes are sizable. For instance, if the $\Lambda(1405)$ is a $\bar{K}N$ bound state, then the amplitude far below the resonance is given not only by the position of the singularity but to a greater extent by the Born term, which indicates a strong dependence on the uncertain interaction range r_o. An old multichannel potential model of Ref. [10] indicates that the available scattering data do not allow one to fix the precise value of r_o. This unfortunate situation is still actual. The r_o is expected to be close to the inverse vector meson mass. However, even though a change of 20% in r_o would not affect the scattering region, it results in a 30% change of f_{KN} in the deep subthreshold region. The corresponding uncertainty in the binding energy then amounts to $\approx$30 MeV. As indicated by few-body calculations of Ref. [11] this problem strongly

*wycech@fuw.edu.pl
†anthony.green@helsinki.fi

affects the outcome. The uncertainties of f_{KN} require further coherent experimental and theoretical studies of $\bar{K}N$ and $\bar{K}$-few-N interactions. It becomes one of the most important purposes of the $\bar{K}$ meson physics.

However, there is one consequence of Eq. (1) that is model independent. If the binding and recoil are so large the f_{KN} amplitudes involve the energies below the thresholds of meson-hyperon decay channels. As a consequence the dominant decay modes are blocked and the lifetimes of nuclear $\bar{K}$ meson systems are determined only by multinucleon captures. This leads to the expectation that such states may live long enough to be detectable [4].

There exists several calculations of $\bar{K}NN$ binding energies. These states are named K^-pp although in reality they correspond to isospin $I_{NN} = 1$ and total isospin $I_{\rm tot} = 1/2$. The first prediction by Akaishi and Yamazaki led to $(E_B, \Gamma) = (48, 60)$ MeV [9], but later versions of this model suggest larger bindings in the 100-MeV region [8]. With a similar, molecular type method, Dote and Weise [12] obtained $E_B <$ 50 MeV and indicated a strong dependence of this result on the short-range NN repulsion. However, the recent three-body calculations based on Faddeev or AGS methods yield larger bindings. Thus Schevchenko *et al.* [13,14] obtained $(E_B, \Gamma) = (55–70, 95–110)$ MeV, whereas Ikeda and Sato [15] calculate $(E_B, \Gamma) = (\sim 80, \sim 73)$ MeV. Later in the text we show that the discrepancy of these two groups of results is due to different $\Lambda(1405)$ properties, explicit description of the multiple scattering in decay channels, and possibly to an incompatible treatment of the NN repulsion.

There are two new elements introduced in this article. First, the P-wave interactions due to $\Sigma(1385)$ have been indicated as a possible source of the strong binding [16]. Here, these are introduced explicitly. Second, the stress is put on the strong $\bar{K}N$ spacial correlations induced by the S- and P-wave resonances.

Leaving aside the interpretation of the peaks attributed to bound $\bar{K}NN$ and $\bar{K}NNN$ systems the essential theoretical questions are:

(i) What is the binding mechanism?
(ii) Are the technical questions under control?
(iii) Can the widths be narrow?

This article attempts to answer these questions and the following results are obtained:

(i) To account properly for the $\bar{K}N$ force range, short-range $\bar{K}N$ correlations, and the NN repulsion, a two-step calculation is performed. First a wave function involving strongly correlated $\bar{K}N$ subsystems is found in a fixed nucleon approximation. This step also allows one to find potentials due to the $\bar{K}$ meson that tend to contract the nucleons. Next, these correlated wave functions and contracting potentials are used as the input in variational calculations for the $\bar{K}$-few nucleon binding. In the $\bar{K}NN$ case the binding energy and width are found by solving the Schrödinger equation.
(ii) Although the dominant mechanism of attraction is related to the $\Lambda(1405)$ state, it is found that another resonant state, the $\Sigma(1385)$, contributes significantly to the structure of the bound states but much less to the binding in $\bar{K}NN$ and $\bar{K}$-few-N systems. In addition the $\Sigma(1385)$ generates new branches of nuclear states that could not be generated by the $\Lambda(1405)$ alone.
(iii) The binding energy is determined to a large extent by the attraction and the repulsive core in NN interactions. With the Argonne NN potential [17] one obtains the lowest state of $\bar{K}NN$ bound by about 40–80 MeV and a $\bar{K}NNN$ state bound by about 90–150 MeV. Moderate dependence on the $\bar{K}N$ interactions is found, provided these are constrained by the shape of $\Lambda(1405)$ and the value of the $\bar{K}N$ scattering length. However, the position of $\Lambda(1405)$ itself is not well known and this becomes the source of a large uncertainty. The effect of $\Sigma(1385)$ on the binding energy is limited, In the states bound via $\Lambda(1405)$ it adds some 5–10 MeV to the $\bar{K}NN$ binding and 10–20 MeV to $\bar{K}NNN$ binding. In this sense the suggestions of Ref. [16] are not fully supported. However, the effect of $\Sigma(1385)$ on the space structure of deeply bound kaonic states is strong. The $\Sigma(1385)$ is formed in peripheral regions and it absorbs a large fraction of the total $\bar{K}$ meson binding. In consequence the radii of these systems are fairly large and the nucleon densities are comparable to those met in the ^{4}He nuclei.
(iv) The problem of uncertainties related to the large recoil momenta entering Eq. (1) is only partly removed. Large kaon momenta are hidden inside the resonant structures. In principle these may be kept under control with the help of other experiments. In practice it is not the case. The other sector of large momenta, due to the strong binding, is partly screened by the short-range NN repulsion. The main consequence is a strong dependence of the meson binding energies on the position of the $\Lambda(1405)$ resonance. In principle the shape of $\Lambda(1405)$ is tested by the invariant mass distribution in the decay $\Sigma\pi$ channel. In practice it is not so as the relevant energy region is located close to the $\Sigma\pi$ threshold. In this region the theoretical and experimental uncertainties are large.
(v) These states are very broad if the binding energies are less than 100 MeV. For stronger bindings, which are possible under the current values of the $\bar{K}N$ parameters the main mesonic decay modes may be closed. The widths for nonmesonic modes are hard to calculate and extrapolations from the emulsion data are not very reliable. New experiments are needed.

A simple physical picture emerges from this approach. The mesons are strongly correlated to slowly moving nucleons. The correlations are of the $\Lambda(1405)$ type at large densities and of the $\Sigma(1385)$ type in the peripheries. Each $\bar{K}N$ pair has a good chance to stay also in the $\Sigma\pi$ form. The structure is rather loose as sizable fractions of the binding energies are hidden in the short-ranged correlations.

II. THE $\bar{K}NN$ BOUND STATE

This section presents an introduction to the method used in this work. Several steps describe the increasing degree of

precision and also the increasing level of technical complications:

(i) At first the $\bar{K}NN$ levels are found within the fixed nucleon approximation with a simple S-wave $\bar{K}N$ interaction.
(ii) The nucleon degrees of freedom and NN interactions are introduced and a related Schrödinger equation is solved.
(iii) The method is extended to multiple channel situations.
(iv) Both S- and P-wave $\bar{K}N$ interactions are allowed.

Consider scattering of a light meson on two identical, heavy nucleons. To begin with, the nucleons are fixed at coordinates $\mathbf{x}_i (i = 1, 2)$ and the wave function is assumed to be in the form

$$\Psi(\mathbf{x}, \mathbf{x}_1, \mathbf{x}_2) = \chi_K(\mathbf{x}; \mathbf{x}_1, \mathbf{x}_2)\, \chi_{NN}(\mathbf{x}_1, \mathbf{x}_2), \tag{2}$$

where $\mathbf{x}$ is the meson coordinate. The notation is simplified and some possible indices are suppressed. The meson wave function χ_K is given by the solution of the multiple-scattering equation

$$\chi_K(\mathbf{x}, \mathbf{x}_1, \mathbf{x}_2) = \chi_K(\mathbf{x})^o - \Sigma_i \int \mathbf{dy} \frac{\exp[ip|\mathbf{x} - \mathbf{y}|]}{4\pi|\mathbf{x} - \mathbf{y}|} \times U_{KN}(\mathbf{y}, \mathbf{x}_i)\, \chi_K(\mathbf{y}, \mathbf{x}_1, \mathbf{x}_2) \tag{3}$$

obtained with fixed positions of the nucleons. An equation of similar structure with a zero range meson-nucleon pseudopotential U was used by Brueckner [18] to calculate the scattering length of a meson on two nucleons. For high-energy scattering it was extensively discussed by Foldy and Walecka, who used finite-range separable interactions U [19]. With such interactions equation (3) allows for semianalytic solutions in the NN, and also in few nucleon cases. Here, the method is extended to the bound-state problem. One looks for solutions of Eq. (3) with no incident wave $\chi_K(\mathbf{x})^o$. The momentum p becomes a complex eigenvalue $p(x_i)$ that determines the energy and width of the system for given nucleon positions x_i.

Equation (3) is written in terms of the Klein-Gordon or Schrödinger propagator. The difference arises when the relation of energy and momentum is established. Reasons of simplicity, that will become clear later, favor the nonrelativistic relation in the $\bar{K}N$ center of mass system. Thus, the interaction is presented as $U_{KN} = 2\mu_{KN} V_{KN}$, where μ_{KN} is the reduced mass. Corrections for relativity may be introduced at a later stage. The potential V_{KN} for an S-wave interaction is chosen in a separable form

$$V_{KN}(\mathbf{x} - \mathbf{x_i}, \mathbf{x}' - \mathbf{x_i}) = \lambda\, \upsilon(\mathbf{x} - \mathbf{x_i})\, \upsilon(\mathbf{x}' - \mathbf{x_i}), \tag{4}$$

where υ is a form factor and λ is a strength parameter. The eigenvalue equation is now reduced to

$$\chi_K(\mathbf{x}, \mathbf{x}_1, \mathbf{x}_2) + \Sigma_i \lambda \int \mathbf{dy} \frac{\exp[ip(\mathbf{x}_1, \mathbf{x}_2)|\mathbf{x} - \mathbf{y}|]}{4\pi|\mathbf{x} - \mathbf{y}|} \upsilon(\mathbf{y} - \mathbf{x_i}) \times \int \mathbf{dy}'\, \upsilon(\mathbf{y}' - \mathbf{x_i})\, \chi_K(\mathbf{y}', \mathbf{x}_1, \mathbf{x}_2) = 0. \tag{5}$$

Equation (5) becomes a matrix equation for wave amplitudes ψ_i defined at each scatterer i by

$$\psi_i = \lambda \int \mathbf{dx}\, \upsilon(\mathbf{x} - \mathbf{x}_i)\, \chi_K(\mathbf{x}, \mathbf{x}_1, \mathbf{x}_2). \tag{6}$$

To find the equations for ψ_i one introduces the off-shell $\bar{K}N$ scattering matrices f and matrix elements of the propagator

$$G_{i,j}(\mathbf{x_i}, \mathbf{x_j}) = \int \mathbf{dy}\, \mathbf{dx}\, \upsilon(\mathbf{x} - \mathbf{x}_i) \frac{\exp(ik|\mathbf{x} - \mathbf{y}|)}{4\pi|\mathbf{x} - \mathbf{y}|} \upsilon(\mathbf{y} - \mathbf{x}_j). \tag{7}$$

The diagonal value, $G_{i,i} \equiv G$, determines the meson-nucleon scattering matrix t by the well-known (see, e.g., Ref. [19]) relation

$$t(E) = (1 + \lambda G)^{-1} \lambda \tag{8}$$

and this yields the full off-shell scattering amplitude f

$$f(k, E, k') = \upsilon(k)\, t(E)\, \upsilon(k'). \tag{9}$$

Here, k, k' are the initial and final momenta, whereas the form factor $\upsilon(k)$ is given by the Fourier transform of $\upsilon(r)$. The Yamaguchi form $\upsilon(k) = 1/(1 + k^2/\kappa^2)$ with a free parameter κ will be used in this article. At zero momenta and at the threshold this choice normalizes f (and t) to the scattering length. Unfortunately, for historical reasons the standard convention in the $\bar{K}N$ system is to define the scattering length by

$$a + ib = -f(k = 0, E = 0, k' = 0) \equiv F(0, 0, 0) \tag{10}$$

and the capital F will be used in several places to comply with the standard $\bar{K}N$ parameters.

To cast Eq. (5) into a standard multiple-scattering equation for ψ_i one carries out the following three steps: (i) integrate Eq. (5) over the i-th form-factor $\upsilon(\mathbf{x} - \mathbf{x_i})$, (ii) select the i-th term from the right-hand side, (iii) multiply Eq. (5) by $(1 + \lambda G)^{-1}$. In this way the kernel of the multiple-scattering equation can be expressed in terms of scattering amplitudes t_i at each nucleon i and propagators describing the passage from the nucleon i to the other nucleon j. One now arrives at a set of linear equations

$$\psi_i + \Sigma_{j \neq i}\, t_j G_{i,j}\, \psi_j = 0, \tag{11}$$

which may be solved numerically. For the Yamaguchi form factors, propagators $G_{i,j}$ allow analytic expressions

$$G_{1,2}(r, k) = \frac{1}{r} \upsilon(k)^2 \left[\exp(ikr) - \exp(-\kappa r) - r \frac{\kappa^2 + k^2}{2\kappa} \exp(-\kappa r) \right] \equiv G(r, k), \tag{12}$$

where $\mathbf{r} = \mathbf{x}_2 - \mathbf{x}_1$. For the sake of illustration, the $\bar{K}NN$ case is presented in some detail. The condition for a bound state with two amplitudes ψ_i leads to a pair of equations

$$\psi_1 + tG\psi_2 = 0, \quad \psi_2 + tG\psi_1 = 0. \tag{13}$$

When the determinant

$$D = 1 - (tG)^2 \tag{14}$$

is put to zero, the binding "momenta" $p(r)$ may be obtained numerically. Two different solutions corresponding to $1 + tG = 0$ or $1 - tG = 0$ may exist. The first solution is symmetric $\psi_2 = \psi_1$ and describes the meson in the S-wave state with respect to the NN center-of-mass. The second

solution is antisymmetric $\psi_2 = -\psi_1$ and describes a P-wave solution. With the rank one separable interaction this latter solution does not exist in the full range of r. However, it arises with the more complicated rank two interactions discussed later.

Eigenvalues corresponding to unstable quasibound states are obtained in the second quadrant of complex $p(r) \equiv p = p_R + ip_I$ plane. In this quadrant the kernel

$$tG = f(p)\Big[\exp(-p_I r)\exp(ip_R r) - \exp(-\kappa r)\Big(1 + r\frac{\kappa^2 - p^2}{2\kappa}\Big)\Big]\Big/ r \qquad (15)$$

is exponentially damped at large distances as required by the asymptotic form of the bound-state wave function χ_K. At short distances G is regularized by the $\bar{K}N$ form factor.

The eigenvalue $p(r)$ determines the energy of the $\bar{K}$ meson bound to the fixed NN pair

$$E = \frac{p(r)^2}{2\mu_{KN}}. \qquad (16)$$

The motivation for this definition of E follows from the example discussed below. If the $\bar{K}N$ interaction is dominated by a quasibound state, such as $\Lambda(1405)$, then the related pole dominates the scattering amplitude and in some energy region $t = \gamma^2/(E - E^*)$, where γ is a coupling constant and $E^* = E_r - i\Gamma_r/2$ is the $\Lambda(1405)$ complex binding energy. The $\bar{K}NN$ eigenvalue $p(r)$ is given by the equation $1 + tG = 0$, which now takes the form

$$E = E^* - \gamma^2 G(r, p). \qquad (17)$$

The solution $E(r) \equiv E_B(r) - i\Gamma(r)/2$ depends on the NN separation r. Because Re $G(r, p)$ close to the resonance is positive, the binding of $\bar{K}$ to fixed NN is stronger than the $\bar{K}$ binding to a nucleon, $|E_B(r)| > |E_r|$. Increasing the separation $r \to \infty$ one obtains $G \to 0$ and $E(r) \to E^*$, i.e., the $\bar{K}$ meson becomes bound to one of the nucleons. In the same limit the lifetime of $\bar{K}$ becomes equal to the lifetime of $\Lambda(1405)$. Hence, the separation energy is understood here as the energy needed to split the $\bar{K}NN$ system into the $\Lambda(1405)N$ system. In the next step of this calculation the nucleon degrees of freedom will be restored. The $r \to \infty$ asymptotic used here must be consistent with the corresponding asymptotic in the Schrödinger equation for $\bar{K}NN$. The condition required is $p(\infty) = q_r$, where q_r is the resonant momentum in the $\bar{K}N$ center-of-mass system, i.e., $q_r^2/2\mu_{KN} = E^*$. Definition (16) fulfills this condition automatically in the nonrelativistic limit.

The difference between the binding at a given separation r and its asymptotic value generates a potential $V_K(r)$, which contracts the nucleons to a smaller radius. It is defined as

$$\text{Re } V_K(r) = E_B(r) - E_B(\infty), \qquad (18)$$

whereas the corresponding imaginary part is

$$\text{Im} V_K(r) = -i\Gamma(r)/2. \qquad (19)$$

A typical profile of $E_B(r)$ is plotted in Fig. 1 as $E_{B,S}$. The asymptotic value $E_B(\infty)$ is obtained at separations $r \geqslant 2$ fm.

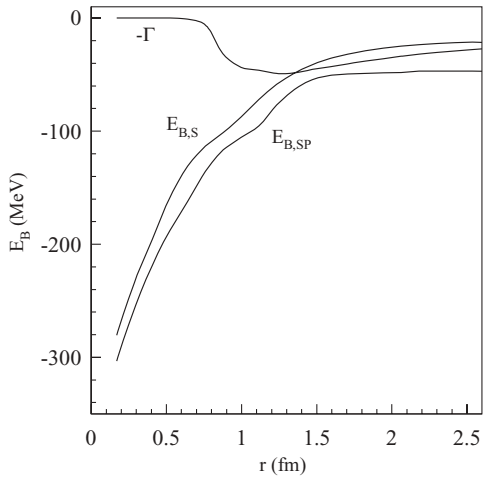

FIG. 1. Binding energies E_B(r) of a $\bar{K} + NN$ pair fixed at a distance r apart in the $I_{NN} = 1$, $I_{KNN} = 1/2$ state with the symmetric meson wave function. The $E_{B,S}$ line shows the binding for the S wave $\bar{K}N$ interactions. The $E_{B,SP}$ one follows from the $S + P$-wave interactions. The upper curve $-\Gamma$ shows 2 Im$E(r)$ for the S-wave case. These results are based on the A. Martin amplitudes [20].

The limits $r \to 0$ in Eqs. (12) and (15) are regular. However, a joint limit of zero-range $\bar{K}N$ interactions, $\kappa \to \infty$, and $r \to 0$ is singular and the $\bar{K}NN$ system collapses. Therefore, some care is necessary when this limit is taken. Here, we stay within a phenomenological approach and the standard expectation that the range of $\bar{K}N$ interactions is determined by vector-meson exchange. In Eq. (12) for G the range of interactions enters twice, first as a cutoff at small distances and second in terms of the form factor $v(k)^2$. We find in a numerical way that these two effects cancel and tG is very stable within the range $3 < \kappa < 6$ fm^{-1}.

A. Schrödinger equation

The solution of the full $\bar{K}NN$ bound-state problem is given by equation

$$\Big(-\frac{\Delta_x}{2m} - \frac{\Delta_1}{2M} - \frac{\Delta_2}{2M} + V_{KN1} + V_{KN2} + V_{NN}\Big)\Psi = E\Psi. \qquad (20)$$

The wave function is assumed in the form $\Psi = \chi_K(x, x_i)\chi_{NN}(r)$ as given in Eq. (2). Multiplying Eq. (20) on the left by χ_K and integrating over the meson coordinate x one obtains the Schrödinger equation for the NN wave function

$$\chi_{NN}(r) = \int \mathbf{dx}\, \chi_K(x, x_i)\Psi(x, x_i) \qquad (21)$$

in the form

$$[-\Delta_1/2M - \Delta_2/2M + V_{NN} + E(r) - E]\chi_{NN} - \Delta E_{\text{kin}}\chi_{NN} = 0. \qquad (22)$$

This is an eigenvalue equation despite the fact that at large distances the "fixed nucleon binding" term $E(r)$ tends to

a constant value that describes the binding of $\bar{K}N$ into $\Lambda(1405)$ in the $\Lambda(1405)N$ asymptotic state. The basic question concerning the asymptotic form of χ_{NN}, i.e., the existence or nonexistence of a $\bar{K}NN$ bound state is determined by the contracting potential $\mathrm{Re}V_K(r)$ defined in Eq. (18). If such a bound state exists, then the total binding is due to both effects—the contracting force and the formation of the asymptotic $\Lambda(1405)$. It has to be added that the structure of $\Lambda(1405)$ changes with decreasing NN separation. Its shape is described by the meson propagator G of Eq. (15). The smaller the NN distance r the larger the eigenvalue $p_I(r)$ and the range of propagation is reduced. In this sense the $\Lambda(1405)$ shrinks in dense nuclear systems.

The last term ΔE_{kin} in Eq. (22) is a correction to the kinetic energies. It is small due to the choice of the meson kinetic energies. In the Schrödinger equation (20) it is given by the meson mass m. However, to determine the $\Lambda(1405)$ properties and to solve the scattering equation (3) the reduced mass μ_{KN} is used. Due to this, the correction term ΔE_{kin} is of the order of $1/M$. In addition, the meson wave function satisfies the relation

$$\Delta_x \chi_K = \sum_i \Delta_i \chi_K, \tag{23}$$

which may be obtained by partial integration over coordinate y in Eq. (5). In this way

$$\Delta E_{\mathrm{kin}} \chi_{NN} = -\frac{1}{M} \Sigma_i \int \mathbf{dx}\, \chi_K \overrightarrow{\partial}_i \chi_K \overrightarrow{\partial}_i \chi_{NN}, \tag{24}$$

which is very small due to angular averaging and sign changes in the derivatives. In more detail this correction reduces to

$$\Delta E_{\mathrm{kin}} \chi_{NN} = -\frac{2}{M} \int d\xi \frac{\xi \mathbf{r}}{\xi r} \frac{G(\xi - \mathbf{r}) \partial_\xi G(\xi)}{\int d\eta [G(\eta - \mathbf{r}) + G(\eta)]^2} \partial_r \chi_{NN}(r), \tag{25}$$

and is suppressed by the angular average over ξ and at large r by the small overlap of $G(\xi - \mathbf{r})$ and $G(\xi)$. The ΔE_{kin} makes a contribution $\approx$0.2 MeV to the binding energy. Such twice-damped, small terms of similar type arise also in more involved versions of this calculation. The ΔE_{kin} is of the same order but is given by very lengthy formulas. Because it is very small in comparison to the dominant uncertainties in V_K it is dropped, leading to a significant simplification of the variational approach.

As the next step, Eq. (22) is solved with an S-wave interaction based on the more realistic NN potential of Argonne [17]. This solution is also compared to another, variational solution with the intention of checking the variational method used in heavier systems. The actual interaction used, in the notation of Ref. [17], has the form

$$v(NN) = v^{\mathrm{EM}}(NN) + v^{\pi}(NN) + v^{R}(NN), \tag{26}$$

where the electromagnetic part v^{EM} includes only the dominant term proportional to $F_C(r)$ in Eq. (4) of Ref. [17], the OPE term v^{π} is given by Eq. (18) of Ref. [17] and the phenomenological short range term v^R from Eq. (20) with the parameters in Table II—again, all from Ref. [17]. This gives directly the S-wave $T = 1$, $S = 0$ interaction $v(S-\mathrm{wave}, T = 1, S = 0)$. However, in the $T = 0$, $S = 1$ deuteron channel, the effect of the tensor interaction $v_t(T = 0, S = 1)$ on the central component $v_c(T = 0, S = 1)$ is incorporated by the closure approximation to give

$$V(S\mathrm{wave, Deuteron}) = v_c(T = 0, S = 1) - \frac{8 v_t(T = 0, S = 1)^2}{\mathrm{Den}}, \tag{27}$$

where the energy denominator was adjusted to $\mathrm{Den} = 338$ MeV to ensure the correct binding energy of the deuteron.

The precision of variational estimates for E (used in the next sections) may be checked against numerical solutions of the Schrödinger equation. It is about 0.3 MeV, compared with the overall binding of $\sim$50 MeV. The width of the state is calculated as

$$\Gamma/2 = -\langle \chi_{NN} | \mathrm{Im} V_K | \chi_{NN} \rangle. \tag{28}$$

B. Interactions in the decay channels

The decay channel $\Sigma\pi$ coupled to the basic $\bar{K}N$ channel is now introduced explicitly. The wave function at each scattering center has two components, one in the $\bar{K}N$ and the other in the $\Sigma\pi$ channel. The scattering amplitudes are two-dimensional vectors $\psi_i \to [\psi_i^K, \psi_i^\pi]$ at each nucleon. Multiple-scattering equations given in the previous section are now changed accordingly. One has

$$\psi_1^K + t^{K,K} G^{K,K} \psi_2^K + t^{K,\pi} G^{\pi,\pi} \psi_2^\pi = 0 \tag{29}$$

$$\psi_1^\pi + G^{\pi,\pi} t^{\pi,\pi} \psi_2^\pi + t^{\pi,K} G^{K,K} \psi_2^K = 0 \tag{30}$$

and an analogous pair with $1 \leftrightarrow 2$. The notation has been changed to describe channel indices and the 2×2 scattering matrix $\hat{f}$. The determinant related to these equations gives the complex eigenvalue $p(x_i)$ in the $\bar{K}N$ channel. The eigenequation is now more complicated. Introducing a new notation in channel indices $U^{a,b} = G^{a,a} t^{a,b}$ the determinant becomes

$$D = [(1 + U^{K,K})(1 + U^{\pi,\pi}) - U^{\pi,K} U^{K,\pi}][(1 - U^{K,K}) \times (1 - U^{\pi,\pi}) - U^{K,\pi} U^{\pi,K}]. \tag{31}$$

The $D = 0$ condition is more transparent close to the singularity in the case of a scattering amplitude given by

$$f^{a,b} \approx \frac{\gamma_a \gamma_b}{E - E_o + i\Gamma/2}. \tag{32}$$

Consistency requires the width to be $\Gamma/2 = p_\pi(\gamma_\pi)^2$, where p_π is the momentum in the decay channel. The singular term (32) permits one to find a solution of Eq. (31) in a fairly simple form. It is presented below in the limit of zero range $\bar{K}N$ (and $\Sigma\pi$) force. The binding energy

$$\mathrm{Re}\ E = E_o - (\gamma_K)^2 \frac{\cos(p_R r)}{r} \exp(-p_I r) - (\gamma_\pi)^2 \frac{\cos(p_\pi r)}{r} \tag{33}$$

becomes larger than the binding of the resonance but the collisions in the decay channel induce oscillations. This

oscillatory behavior is also seen in the width of the system

$$\mathrm{Im}\, E = -(\gamma_\pi)^2 p_\pi \left[1 + \frac{\sin(p_\pi r)}{p_\pi r}\right] - (\gamma_K)^2 \frac{\sin(p_R r)}{r} \exp(-p_I r). \quad (34)$$

The effect of $\bar{K}N$ scattering represented by the second term enlarges the width as p_R is negative. The contribution from multiple scattering in the decay channel is sizable in general but it oscillates and may under some conditions reduce the total width. That is an effect of interference in the decay channel. Scattering in the decay channel turns out to be constructive in the $\bar{K}NN$ case but it is not necessarily so in some heavier systems.

C. *S*- and *P*-wave interactions

With the $\bar{K}N$ interactions allowed in both S and P waves the scattering equation (11) is a $4 \otimes 4$ matrix equation relating four amplitudes ψ_i. The amplitudes for S waves are now denoted by ψ_1^s, ψ_2^s. For P-wave interactions the corresponding amplitudes are vectors. As there is only one vector in the NN system, the relative separation, the P amplitudes are chosen to be $\mathbf{r}\psi_1^p$ and $\mathbf{r}\psi_2^p$. The scattering is now described by three types of propagators $G^{a,b}$ related to consecutive collisions in the (S, S) (S, P), and (P, P) waves. The scattering equations are

$$\psi_1^s + f^s G^{ss} \psi_2^s - f^s G^{\mathrm{sp}} r^2 \psi_2^p = 0 \quad (35)$$

$$\psi_2^s + f^s G^{ss} \psi_1^s + f^s G^{\mathrm{sp}} r^2 \psi_1^p = 0 \quad (36)$$

$$\psi_1^p + f^p G^{pp} \psi_2^p + f^p G^{\mathrm{sp}} \psi_2^s = 0 \quad (37)$$

$$\psi_2^p + f^p G^{pp} \psi_1^p - f^p G^{\mathrm{sp}} \psi_1^s = 0, \quad (38)$$

where the propagation in between two P wave interactions is described by $G^{pp} = G_O^{pp} + r^2 G_T^{pp}$. Indices numbering the nucleons have been suppressed. The propagator G^{ss} is given in Eq. (12) and explicit formulas for G^{sp}, G_O^{pp}, G_T^{pp} may be found in the Appendix. All these functions are regular in the $r \to 0$ limit. The determinant D of this system factorizes into two terms

$$D = D_S D_P, \quad (39)$$

where

$$D_S = (1 + G^{ss} f^s)(1 - G^{pp} f^p) - G^{\mathrm{sp}} r^2 f^s f^p, \quad (40)$$

$$D_P = (1 - G^{ss} f^s)(1 + G^{pp} f^p) - G^{\mathrm{sp}} r^2 f^s f^p. \quad (41)$$

Let us consider the solution of $D_S = 0$ close to the $\Lambda(1405)$ resonance. It is given by an equation analogous to (17)

$$E = E^* - b^2 G^{ss}[r, p(E)] \left[1 - \frac{r^2 (G^{\mathrm{sp}})^2 f^p}{1 - G^{pp} f^p}\right]. \quad (42)$$

The second term in parentheses describes the effect of P-wave interactions. At energies below $\Sigma(1385)$ the amplitude f^p is negative and generates an additional attraction.

Isospin symmetry simplifies the algebraic structure of the scattering equations which are (see next sections) expressed by appropriate isospin combinations of the isospin $\bar{K}N$ scattering amplitudes f. Equations (35)–(38) allow for a simple symmetry of the total $\bar{K}NN$ wave function. Thus, under the eigenvalue condition (40) the coordinate wave function becomes symmetric with respect to the exchange of nucleon coordinates. This condition allows solutions in terms of two amplitudes $\psi^s = \psi_1^s = \psi_2^s$ and $\psi^p = \psi_1^p = -\psi_2^p$. Wave functions for the $\bar{K}NN$ system have the form

$$\Psi(\mathbf{r}, \mathbf{x}) = \chi_{NN}(r)[G(\mathbf{x} - \mathbf{r}/2) + G(\mathbf{x} + \mathbf{r}/2)]\psi_s + \chi_{NN}(r) \times \overrightarrow{r}\, \overrightarrow{\partial}_x [G(\mathbf{x} - \mathbf{r}/2) - G(\mathbf{x} + \mathbf{r}/2)]\psi_p, \quad (43)$$

where $\mathbf{x}$ is the meson coordinate in the NN center-of-mass system and $\chi_{NN}(r)$ is the NN wave function. To make this formula more transparent the zero-range force limit is taken. The two terms in Eq. (43) follow the $\bar{K}N$ interactions in S and P waves. The weight of the P-wave contribution is given by

$$\frac{\psi_p}{\psi_s} = \frac{f^p G^{\mathrm{sp}}}{1 - f^p G^{pp}}, \quad (44)$$

which becomes dominant close to the zero of the denominator in this equation. At large NN separations it happens almost at the singularity in f_p. In this region the lowest energy, symmetric, solution of $D_S = 0$ is given essentially by the situation $1 - G^{pp} f^p \approx 0$. Such a solution exists for $r \geqslant 1.6$ fm in the proper quadrant of the complex momentum. This implies that, at large separations, it is energetically profitable for the $\bar{K}NN$ system to exist in the $N\ \Sigma(1385)$ configuration, with the nucleon and $\Sigma(1385)$ weakly repelling each other. At shorter distances the condition $1 + G^{ss} f^s \approx 0$ determines the attraction generated by $\Lambda(1405)$. Despite repulsive effects of the P-wave interaction such a solution yields the strongest binding, because a large piece of the binding energy is hidden within the structure of $\Sigma(1385)$.

The $\bar{K}NN$ system is built on short range $\bar{K}N$ and NN correlations and the $\Psi(\mathbf{r}, \mathbf{x})$ contains a large number of partial waves coupled to zero total angular momentum. In Jacobi coordinates (r, s) the $L_r \otimes L_s$ decomposition of the first term of $\Psi(\mathbf{r}, \mathbf{x})$ is mainly $S \otimes S$. Both terms involve even values of L_r and the spin-isospin structure of the NN pair is either $I_{NN} = 0$, $S_{NN} = 1$ or $I_{NN} = 1$, $S_{NN} = 0$. Both types of states may be formed.

Other solutions are determined by $D_P = 0$. This condition allows amplitudes of different symmetry $\psi^s = \psi_1^s = -\psi_2^s$ and $\psi^p = \psi_1^p = \psi_2^p$. In comparison with Eq. (43), the wave functions for the $\bar{K}NN$ system

$$\Psi(\mathbf{r}, \mathbf{x}) = \chi_{NN}(r)[G(\mathbf{x} - \mathbf{r}/2) - G(\mathbf{x} + \mathbf{r}/2)]\psi_s + \chi_{NN}(r) \times \overrightarrow{r}\, \overrightarrow{\partial}_x [G(\mathbf{x} - \mathbf{r}/2) + G(\mathbf{x} + \mathbf{r}/2)]\psi_p \quad (45)$$

are now antisymmetric in the nucleon coordinates and contain odd angular momenta L_r, L_s in the $L_r \otimes L_s$ decomposition. The spin-isospin structure of the NN pair is either $I_{NN} = 0$, $S_{NN} = 0$ or $I_{NN} = 1$, $S_{NN} = 1$. The NN interactions in the $I_{NN} = 0$, $S_{NN} = 0$ states are repulsive and do not support any $\bar{K}NN$ bound states. However, $I_{NN} = 1$, $S_{NN} = 1$ states may be formed.

The results of the two previous subsections may be unified. The notation used in Eq. (31) is now extended to include the partial wave index in channel $\bar{K}N$: $U^{p,s} = G^{p,p} t^s$, $U^{s,p} = G^{s,s} t^p$, $U^{p,p} = G^{p,p} t^p$, $U^{s,s} \equiv U^{K,K}$. The last equivalence

indicates that the P-wave multiple scattering is included only in the basic $\bar{K}N$ channel. For the determinant of scattering equations one obtains $D = D_S D_P$ where now

$$D_S = [(1+U^{K,K})(1+U^{\pi,\pi}) - U^{\pi,K}U^{K,\pi}](1+U^{p,p}) - [(1-U^{\pi,\pi})U^{p,s}U^{s,p}] \quad (46)$$

$$D_P = [(1-U^{K,K})(1-U^{\pi,\pi}) - U^{\pi,K}U^{K,\pi}](1+U^{p,p}) - [(1+U^{\pi,\pi})U^{p,s}U^{s,p}]. \quad (47)$$

The solutions of the corresponding eigenvalue equations retain the symmetries indicated in the previous section.

The addition of $\bar{K}N$ P-wave interactions changes the asymptotics. The lowest separation energy is now due to $\bar{K}NN \to \Sigma(1385)N$ because the $\Sigma(1385)$ mass is smaller than the $\Lambda(1405)$ mass. The difference is visualized in Fig. 1, which indicates typical binding energies $E(r)$ for the symmetric solutions. For the S-wave $\bar{K}N$ interaction, the energy, denoted by $E_{B,S}$, reproduces the separation energy related to the $\bar{K}NN \to \Lambda(1405)N$ asymptotics. In the case of S and P interactions the binding energy (denoted by $E_{B,SP}$) reflects the $\Sigma(1385)N$ asymptotic state. Let us notice, however, that the contracting potentials $E_B(r) - E_B(\infty)$ are very similar in both situations. Thus the main effect of the $\Sigma(1385)N$ is to provide stronger binding due to the $\Sigma(1385)$ type of correlations formed predominantly at large internucleon distances.

III. $\bar{K}N$ INTERACTIONS

The coupled multichannel $\bar{K}N, \Sigma\pi, \Lambda\pi$ system is the easiest to describe in terms of the $\hat{K}$ matrix related to the scattering matrix $\hat{T}$ by the algebraic Heitler equation

$$\hat{T} = \hat{K} - \hat{K} i \hat{Q} \hat{T}, \quad (48)$$

where Q is a diagonal matrix of channel momenta in the center-of-mass system. Early parametrizations involved constant K-matrix elements chosen to fit the scattering data. Later these were improved by an effective range expansion. As the data were (and still are) poor such fits were supplemented by additional consistency conditions formulated in terms of dispersion relations [20,21]. Such solutions can be tested above the $\bar{K}N$ threshold and to some extent in the $\Sigma\pi$ channel. For the dominant isospin 0 interactions there are two types of solutions. These are given in Table I in terms of the inverse $\hat{M} = \hat{K}^{-1}$ matrix that in turn determines the scattering matrix

$$\hat{T}^{-1} = \hat{M} + i\hat{Q}. \quad (49)$$

Extrapolations into the complex energy plane display a similar $\Lambda(1405)$ pole position. However, the physics in both solutions indicates different interplay of the main $\bar{K}N$ with the hyperon pion channels. The position of the singularity is given essentially by the attractive and, in both cases, large $K_{KN,KN}$ element. This allows one to interpret $\Lambda(1405)$ as a $\bar{K}N$ quasibound state. In principle there exists an alternative possibility—the Λ as a quark state. If this is the case it may be introduced into the K matrix as an external pole in $\hat{K} \sim 1/(E - E^*)$. However, the scattering data exclude such a term or limit it to a very small contribution [20]. Amplitudes below the $\bar{K}N$ threshold may be tested indirectly, either in the elastic $\Sigma\pi$ channel or in the $\bar{K}N \to \Sigma\pi$ transitions on bound nucleons [33]. These reactions support the bound-state interpretation but are not very restrictive on the position of the singularity. In particular, the analysis of Dalitz and Deloff [23] shows that several models offer comparable descriptions of the $\Sigma\pi$ data in the resonance region. The M-matrix model given in the DD column of Table I is only slightly favored by the authors of Ref. [23].[1]

The KWW column in Table I comes from a quasirelativistic separable potential model. It belongs to a second type of solutions and was based on the B. Martin-Sakitt solution. The

[1]We thank Andrzej Deloff for supplying amplitudes of the DD model.

TABLE I. The semiphenomenological $I = 0$ $\bar{K}N$ scattering parameters. First three lines give M matrices at the $\bar{K}N$ threshold (fm^{-1}). Next two lines give the $\Lambda(1405)$ pole position ($E^*, \Gamma/2$) in the complex energy plane (MeV). The $\bar{K}N$ scattering length $a_o + ib_o$ and amplitudes at 100 MeV below the threshold Re $F_{-100} + i$ImF_{-100} are given in units of fm. The next column KWW* corresponds to the KWW model modified to change the $\Lambda(1405)$ parameters. The first solution AM, will be referred to as type one, and the solutions BM, DD, KWW, and KWW* as type two. The AY column shows results from a potential model of Ref. [34] while the last column shows typical results from the chiral SU(3) approach. The F_{-100} amplitudes in the last two columns marked by $\sim$ are taken from Fig. 15 of Ref. [27] and may not be very precise. The HW model generates two poles as indicated below and discussed in the text.

Solution	AM [20]	BM [21]	DD [23]	KWW [10]	KWW*	AY [34]	HW [27]
$M_{KN,KN}$	−0.07	−1.21	−1.136	−1.27	−1.27		
$M_{KN,\pi\Sigma}$	−1.02	1.53	1.254	1.50	1.50		
$M_{\pi\Sigma,\pi\Sigma}$	1.94	−3.05	−2.205	−3.05	−3.05		
E^*	1411	1415	1404.9	1409	1405	1406	1428,1400
$\Gamma/2$	17	13	26.6	22	24	25	17,76
a_o	−1.70	−1.55	−1.54	−1.52	−1.52	−1.70	
b_o	0.68	0.58	0.74	0.60	0.60	0.68	
Re F_{-100}	−2.34	−1.33	−8.132	−2.64	−5.38	~ -4.4	~ -1.2
ImF_{-100}	0.10	0.06	1.11	0.22	0.86	∼2.1	∼0.2

KKW model is successful in the reproduction of the kaonic hydrogen atom $1S$ level shift and width. The old prediction [24]: $\Delta E = 0.33$ keV (repulsion) and $\Gamma = 0.26$ keV compares very well with the average of two experimental results by KEK ($\Delta E = 323 \pm 63 \pm 11$ eV $\Gamma = 407 \pm 208 \pm 100$ eV) [25] and by DEAR ($\Delta E = 193 \pm 37 \pm 6$eV $\Gamma = 247 \pm 111 \pm 30$ eV) [26]. This model is extended here by a small change of the range parameter (and related change in effective range) with the intention to move the $\Lambda(1405)$ position to the PDG recommended 1405 MeV. As shown in Ref. [10] the results above the $\bar{K}N$ threshold are essentially the same. The elastic amplitudes obtained in this way are very close to the recent version of the Yamazaki and Akaishi phenomenological local potential approach (the [AY] entry in Table I). In the $K^- pp$ system, where comparison is possible, the KKW* and AY models give similar binding energies and widths.

The last entry in Table I indicates a few properties of SU(3) chiral models. The results of Hyodo and Weise [27] are presented although this model is also developed by other groups [28,29]. The results differ dramatically from the phenomenological description. The main difference is that the basic $\Sigma\pi$ interaction is strongly attractive in the chiral SU(3) model, repulsive in most of the phenomenological approaches (BM, KKW, DD, other models in Ref. [23]) or negligible (YA). As a consequence the chiral model generates a broad resonance in the $\Sigma\pi$ channel which takes away the strength of interaction in the $\bar{K}N$ channel. The $\Lambda(1405)$ state becomes weakly bound and weakly coupled. Subthreshold $\bar{K}N$ scattering amplitudes are smaller and the $K^- pp$ system is weakly bound [12].

The selection of the correct model description is difficult due to the low quality of the old scattering data. The standard test of the $\Lambda(1405)$ profile is the shape of the $\Sigma\pi$ mass spectrum. However, as shown in Ref. [23], several models of the type two give very good representation of this spectrum. The chiral models are perhaps less successful but as rightly argued in Ref. [27], the data do not represent pure isospin 0 state. At this point we suggest another check—the measurement of the $K^- p \to \Sigma^- \pi^+$ /$K^- p \to \Sigma^+ \pi^-$ ratio that is strongly energy dependent in the subthreshold region. Some otherwise unpublished nuclear data of Keane exist in Ref. [33], where this problem is discussed.

A. The separable off-shell extension

The three-channel or two-channel separable model is used here to extend the phenomenological S-wave $\bar{K}N$ interactions off the energy shell. This method is standard in momentum space but here we have already used the coordinate representation. In a single $\bar{K}N$ channel case the potential equivalent to those of Eq. (3) is described by

$$V(k, k') = \lambda v(k) v(k'). \tag{50}$$

The Yamaguchi form factors $v(k) = \kappa^2/(\kappa^2 + k^2)$ are convenient to perform explicit analytic calculations in both representations. The related Fourier transforms are of Yukawa form $v(r) = \kappa^2 \exp(-\kappa r)/(4\pi r)$ and are normalized to δ functions in the limit of zero range forces. The off-shell scattering amplitude becomes

$$f_{KN} = \frac{v(k) v(k')}{\lambda^{-1} + G(E)}. \tag{51}$$

With the nonrelativistic form of the kinetic energy $E_{\rm kin} = q^2/(2\mu_{KN})$ one obtains

$$G(E) = \int d\tau \frac{v(t)^2}{2\pi^2(\tau^2 - q^2)} = \frac{\kappa}{2(1 - iq/\kappa)^2}. \tag{52}$$

At the $\bar{K}N$ threshold energy $E_t = M_K + M_N$, the standard convention requires one to define the scattering length as $a_o + ib_o = -f_{KN}(E_t)$. Below the threshold $1/\lambda + G$ is forced to have a zero corresponding to the $\Lambda(1405)$ state. The complex momentum at this point is

$$p_B = \left(\frac{\lambda_S \kappa^3}{2}\right)^{1/2} - \kappa. \tag{53}$$

The next step to improve the absorptive part is to guarantee that it vanishes below the $\Sigma\pi$ threshold. That is achieved by scaling the absorption strength Imλ by a phase-space factor $f_\varrho = q_{\Sigma\pi}(E)/q_{\Sigma\pi}(E_t)$, where $q_{\Sigma\pi}$ is the momentum in the decay channel. The values $\lambda_S = -0.602 \exp(i\, 0.12\, f_\varrho)$ fm and $\kappa = 4.5$ fm^{-1} give a good reproduction of the PDG recommended $E = 1405$ and $\Gamma = 50$ MeV values [23,32].

This one channel amplitude may serve as a guide, but to describe finer details and for a better comparison with the scattering data one needs multichannel separable models. Below, two types of multi-channel reaction matrices are extrapolated off the energy-shell.

(i) One solution has been given by Krzyzanowski *et al.* [10] in terms of a quasirelativistic multichannel separable potential. The $G(E)$ used there differs from the solution (52) by an invariant momentum phase space and the use of quasirelativistic intermediate meson energies $E = q^2/(2M_N) + \sqrt{m^2 + q^2}$. This solution was motivated by the early B. Martin and Sakitt [21] K matrix (BM in Table I) and as may be seen in this table it offers similar on-shell parameters.

(ii) Another solution is based on the commonly used A. Martin's K matrix [20]. However, in the decay channels this matrix is not well reproduced by simple rank one separable potentials. Instead, we use the extrapolation $K^{\rm off}(k, E, k') = v(k) K^{\rm on} v(k')$, with the Yamaguchi form factors and $\kappa = 4.5$ fm^{-1} as obtained above in the one-channel case.

B. *P*-wave meson-nucleon interactions

To account for the P-wave interactions dominated by $\Sigma(1385)$ the scattering amplitude of Eq. (9) is generalized to

$$f_{KN} = f_S + f_P = f_S + 2\, \mathbf{k}\mathbf{k}'\, f_P^{l+}. \tag{54}$$

The last term is a consequence of the $j = l + 1/2$ total spin of $\Sigma(1385)$. It involves an $l + 1$ factor instead of $2l + 1$ typical for spin-zero situations. The omitted piece contains spin-flip amplitudes and is expected to be small in the few-body context. The f_P^{l+} term is described here by a separable

single-channel K matrix that in the $\bar{K}N$ channel is given by

$$K(\mathbf{k},\mathbf{k}') = \gamma_K^2 \frac{\mathbf{k}\mathbf{k}' v_P(k) v_P(k')}{E - E_o + i\Gamma_\pi/2}, \tag{55}$$

where the form factor is

$$v_P(k) = \frac{\kappa^4}{(\kappa^2 + k^2)^2}, \tag{56}$$

and E_o is a phenomenological parameter that determines the position of $\Sigma(1385)$. The width Γ_π is strongly energy dependent:

$$\Gamma_\pi = \gamma_{\Lambda\pi}^2 q_{\Lambda\pi}^3 + \gamma_{\Sigma\pi}^2 q_{\Sigma\pi}^3. \tag{57}$$

In these equations the q's are the channel momenta and γ are couplings of the resonance to the $\Sigma\pi$ and $\Lambda\pi$ channels. The latter are determined by the experimental decay width of about 36($\pm$2) MeV and the $\Sigma\pi$ branching ratio of 0.13($\pm$0.01) [32]. For the coupling to the $\bar{K}N$ channel the SU(3) value $\gamma_{KN}^2/\gamma_{\Sigma\pi}^2 = 2/3$ is taken. This value is consistent with the experimental result of Brown, which yields 0.57($\pm$0.18) [30].

The coupling to the $\bar{K}N$ channel generates the off-shell scattering amplitude

$$f_P(\mathbf{k}, E, \mathbf{k}') = \frac{2\mathbf{k}\mathbf{k}' v_P(k) v_P(k') \gamma_{KN}^2}{E - E_o + \gamma_{KN}^2 \int \frac{d\tau \tau^2 v_P(\tau)^2}{2\pi^2(\tau^2 - k_{KN}^2)} + i\Gamma_\pi/2}$$
$$\equiv \mathbf{k}\mathbf{k}' v_P(k) f_P(E) v_P(k'). \tag{58}$$

Let us notice that below the KN threshold the integral in Eq. (58) deforms significantly the shape of the resonance profile. The range parameter $\kappa = 3.8$ fm^{-1} and $E_o = 1505.2$ MeV are used to reproduces the profile tested experimentally by Cameron *et al.* [31] in the $\Lambda\pi$ channel. For further applications the coordinate representation is needed, which is given by equation

$$f(\mathbf{x}, E, \mathbf{x}') = \lambda_P \overleftarrow{\partial}\, v_P(x) f_P(E) v_P(x') \overrightarrow{\partial} \tag{59}$$

in terms of the Fourier transforms of form factors (56).

IV. FEW-NUCLEON SYSTEMS

The procedure presented in the $\bar{K}NN$ section is now extended to systems consisting of several nucleons. Practical calculations are done for three and four nucleons. At first the multiple-scattering equations similar to Eqs. (3)–(5) in the previous section are solved in fixed nucleon systems. The bound K-meson wave function χ_K is a solution of

$$\chi_K(\mathbf{x}, x_1 \cdots x_n) = -\Sigma_i \Sigma_\beta \int \mathbf{dy} \frac{\exp(ik|\mathbf{x}-\mathbf{y}|)}{4\pi|\mathbf{x}-\mathbf{y}|} v(\mathbf{x}-\mathbf{x}_i)_\alpha$$
$$\times \lambda^{\alpha\beta} v(\mathbf{y}-\mathbf{x}_i)_\beta \, \chi_K(\mathbf{y}, x_1 \cdots x_n), \tag{60}$$

where indices α, β denote channels and partial waves of the meson-baryon pair. An index related to the symmetry of χ is suppressed. By analogy with Eqs. (6) and (7), Eq. (60) may be reduced to a matrix equation for the wave amplitudes defined at each scatterer as

$$\psi_i^\alpha = \Sigma_\beta \int \mathbf{dy}\, \lambda^{\alpha\beta} v(\mathbf{y}-\mathbf{x}_i)_\beta \, \chi_K(\mathbf{y}, x_i). \tag{61}$$

The kernel of the scattering equation can be now expressed in terms of scattering amplitudes $f_i^{\alpha,\beta}$ at each nucleon i and propagators describing the passage from nucleon i to another nucleon j. The latter are given by

$$G_{i,j}^{\alpha,\beta} = \int \mathbf{dy}\, \mathbf{dx}\, v(\mathbf{x}-\mathbf{x}_i)_\alpha \frac{\exp(ik|\mathbf{x}-\mathbf{y}|)}{4\pi|\mathbf{x}-\mathbf{y}|} v(\mathbf{y}-\mathbf{x}_j)_\beta. \tag{62}$$

The procedure explained in Sec. II leads to a set of linear equations

$$\psi_i^\alpha + \Sigma_{\beta\gamma} \Sigma_{j\neq i} f_j^{\alpha,\beta} G_{i,j}^{\beta\gamma} \psi_j^\gamma = 0, \tag{63}$$

which are solved numerically. This matrix equation is simplified as the G's are diagonal in channel indices and the f are diagonal in the partial wave index. Still, the corresponding determinants are complicated algebraic expressions involving functions G and f. Numerical solutions become a difficult problem. It has been solved in the following approximate way. The determinant consists of many terms that are arranged according to the number of collisions. With up to four collisions in the main channel we retain the structure found in the $\bar{K}NN$ situation and the determinant D of this system is presented as

$$D = 1 + \Sigma_{\text{pairs}}(D_S D_P - 1) + O_{\text{higher orders}}, \tag{64}$$

where D_S and D_P are defined in Eqs. (46) and (47). The main term is composed of collisions in the $\bar{K}NN$ subsystems that allows one to keep track of the wave function symmetry. The terms of higher order in f are dropped.

The solution of the full $\bar{K}$-few-N bound-state problem is given by the equation

$$\left[E + \frac{\Delta_x}{2m} + \sum_i \frac{\Delta_i}{2M} - \sum_i V_{KN_i} - \sum_{i,j} V_{N_i N_j}\right] \Psi(x, x_1, \ldots, x_n) = 0. \tag{65}$$

Again we assume the wave function to be given by Eqs. (2) and (60), i.e., $\chi_K(x, x_1 \cdots x_n)\chi_N(x_1, \ldots, x_n)$. Projecting Eq. (65) on ψ_K one obtains the Schrödinger equation for the few-nucleon wave function

$$\chi_N(x_i) = \int \mathbf{dx}\, \chi_K(x, x_i) \Psi(x, x_i) \tag{66}$$

in the form

$$\left[E - E^c(x_i) + \sum_i \frac{\Delta_i}{2M} - \sum V_{NN}\right] \chi_N + \Delta E_{\text{kin}} \chi_N = 0, \tag{67}$$

where ΔE_{kin} is a correction to the nucleon kinetic energies. As in Eq. (24) it is given by

$$\Delta E_{\text{kin}} \chi_N = -\frac{1}{M} \Sigma_i \int \mathbf{dx}\, \partial_i \psi_K \partial_i \Psi \tag{68}$$

and as before turns out to be very small due to angular averaging and sign changes in both the derivatives. As discussed in the $\bar{K}NN$ situation this correction has been dropped. In deriving equation (67) a special form (60) of the

meson wave function is used. As in Eq. (23) it satisfies the relation

$$\Delta_x \chi_K = \sum_i \Delta_i \chi_K. \tag{69}$$

In the next step, equation (67) is solved by a variational method with the NN potential of Argonne [17]. The trial wave function is of the form

$$\chi_N = \prod_{i,j,i\neq j} \left[1 - \exp\left(-\lambda_c^2(\mathbf{x}_i - \mathbf{x}_j)^2\right)\right] \times \exp(-\lambda_l|\mathbf{x}_i - \mathbf{x}_j|)/|\mathbf{x}_i - \mathbf{x}_j|, \tag{70}$$

where λ_c, λ_l are variational parameters. This form is chosen to give the correct asymptotic limit for large $|\mathbf{x}_i - \mathbf{x}_j|$ and also gives a vanishing wave function for small $|\mathbf{x}_i - \mathbf{x}_j|$ as expected for a strong repulsion in the NN potential.

V. RESULTS

A. $\bar{K}NN$

In this section the calculations of $\bar{K}NN$ levels are presented. The sensitivity to $\bar{K}N$ input parameters is studied and the states of different symmetry are discussed.

Contracting potentials $V_K(r)$ were calculated with several solutions for the phenomenological S-wave $\bar{K}N$ reaction matrices presented in Table I. The solutions of second type may be well fitted with a rank one separable potential. Here, the calculations are done with the quasirelativistic model of Ref. [10]. This model is based on the K matrix of B. Martin [21]. Numerically it is fairly close to the separable potential of Ref. [22]. For the first type of solutions in Table I, due to A. Martin [20] no satisfactory rank one separable approximation is found. This difficulty is related to the large effective range parameters involved in this K matrix. To retain the physics involved, a simple off-shell extension is adopted $K_{i,j} \to v(k_i)K_{i,j}v(k_j)$. The Yamaguchi form factors have been used and the inverse range parameter κ was varied over the range of 3–6 fm^{-1}. The actual value of κ affects the multiple scattering via propagator $G_{ss}(k,r)$ of Eq. (12). Larger values reduce the form factor $v(k)$ but enhance the significance of the small r region in $G_{ss}(k,r)$. On average these two effects balance very well and one finds a very weak ($\sim$1 MeV) dependence of the total binding energy on the actual value of κ. The results given in Fig. 1 and in the tables that follow are obtained with $\kappa = 4.5$ fm^{-1}.

The energies of the most strongly bound $\bar{K}NN$, $I_{\rm tot} = 1/2$, $I_{NN} = 1$, quasibound states are given in Tables II and III. The first table describes several steps of the approximation, whereas the second table indicates the dependence of binding on the $\bar{K}N$ input parameters.

The first line in Table II is determined essentially by the effects of $\Lambda(1405)$ excitations described in the elastic channel only. The second line describes additional effects due to multiple scattering in the $\Sigma\pi$ channel. The other two lines include the P-wave interactions. The energies of $I_{\rm tot} = 1/2$, $I_{NN} = 1$ states given by the S-wave interactions and described by multiple scattering in the single, $\bar{K}N$, channel span the region of 30–50 MeV. These results are consistent with the findings of Akaishi and Yamazaki [9] and Dote and Weise [12] obtained with different methods. The differences within this range are due to a different $\bar{K}N$ and/or NN input. As seen in the second and fourth rows, significant changes arise with the explicit inclusion of the multiple scattering in the $\Sigma\pi$ channels. The binding rises by 10 to 20 MeV and the effect of collision broadening is large.

TABLE II. Binding energies and widths (in MeV) of the $\bar{K}NN$, $I_{\rm tot} = 1/2$, $I_{NN} = 1$ space-symmetric states. The results on the left are based on AM parameters, and the results on the right follow KWW parameters discussed in Table I. The first column specifies the channels explicitly involved in the multiple-scattering and meson-nucleon partial waves. $R_{\rm rms}$ is the radius mean squared of the NN separation (in fm). The last line is obtained with the simplest separable potential discussed in the text and the $I_{KN} = 1$ amplitudes from AM.

Solution	AM [20]			KWW [10]		
	E_B	Γ	$R_{\rm rms}$	E_B	Γ	$R_{\rm rms}$
$\bar{K}N;\ S$	27	36	3.1	35.5	37	2.4
$\bar{K}N, \Sigma\pi; S$	37	42	2.5	43.1	47	2.1
$\bar{K}N; S, P$	49	36	3.7	49.7	36	3.3
$\bar{K}N, \Sigma\pi; S, P$	52	37	2.9	56.5	39	2.3
$\bar{K}N; S$	47	47	2.3			

Table III shows binding energies obtained with the "canonical" Λ pole position $E = 1405$ MeV [23,32] that is lower than the position obtained in other parametrizations. The result given in the second line of this table is comparable to the results obtained, with a similar input, by Schevchenko *et al.* [13]. The latter work employs a superior Faddeev technique, but a more detailed comparison of results is not easy because that calculation uses a rank one separable potential to describe the NN interactions.

The same position of the Λ pole is used by Yamazaki and Akaishi. In the recent calculation [34] these authors find similar deeply bound states. It is also shown there that the strength of the repulsive NN core has a limited effect on these binding energies. We confirm this finding. With the method used here this is due to the shrinking of the meson propagation range for

TABLE III. Binding energies and widths (in MeV) of the $\bar{K}NN$, $I_{\rm tot} = 1/2$, $I_{NN} = 1$ space-symmetric states. These results are based on KWW [10] parameters modified to set the pole of $\Lambda(1405)$ at 1405 MeV and the width at 48 MeV and given in Table I (KWW*). The first column specifies the channels explicitly involved in the multiple scattering and the meson-nucleon partial waves. $R_{\rm rms}$ is the radius mean squared of the NN separation (in fm).

Solution	KWW*		
	E_B	Γ	$R_{\rm rms}$
$\bar{K}N; S$	50	51	2.05
$\bar{K}N, \Sigma\pi; S$	71	85	1.81
$\bar{K}N; S, P$	65	43	2.09
$\bar{K}N, \Sigma\pi; S, P$	78	60	1.88

TABLE IV. Binding energy and width (in MeV) of the $\bar{K}NN$, $I_{\rm tot} = 1/2$, $I_{NN} = 0$ space-symmetric states. Results on the left are based on A. Martin parameters and do not support a bound state (no b.s.). The results on the right follow the KWW parameters. This result involves $S + P$-wave interactions and external interactions in two meson-nucleon channels. $R_{\rm rms}$ is the radius mean squared of the NN separation (in fm).

E_B	Γ	$R_{\rm rms}$	E_B	Γ	$R_{\rm rms}$
no b.s.	–	–	47.1	36	∼7

short NN separations. Presumably the same happens when a separable NN interaction is used in the Faddeev equations.

The inclusion of resonant P-wave interactions increases the binding by some 10 MeV. There is some room for different values as the experimental $\bar{K}N\Sigma(1385)$ coupling is not certain. However, the main effect of $\Sigma(1385)$ is a change of structure in the $\bar{K}NN$ systems. A sizable portion of the binding energy is contained in the structure of this resonance. However, the system is dissolved as the inclusion of P waves enlarges the NN separation and the formation of $\Sigma(1385)$ is essentially a peripheral effect. The $\bar{K}N$ correlations for $r > 1.6$ fm are mostly of the $\Sigma(1385)$ type. The other effect of P-wave interactions is a formation of additional $\bar{K}NN$ states. These are given in Tables IV and V and discussed below.

The energies of $\bar{K}NN$ quasibound states with $I_{NN} = 0$ given in Table IV are determined essentially by the $\Sigma(1385)$ excitations. Let us notice that the result is unstable against the $\bar{K}N$ input. The state is still more likely to exist with a lower value of the $\Lambda(1405)$ energy. In any case it is a very loose structure that might be a quasibound or a virtual state.

The energy of an asymmetric quasibound state is given in Table V. It is determined essentially by the $\Sigma(1385)$ excitations. The table in Appendix B indicates that the K^-nn state has the largest possible Σ component that offers the strongest $\Sigma(1385)N$ attractive potential. It reaches a maximum depth of about -10 MeV at a distance of 1 fm, but it is not strong enough to overcome the NN P-wave barrier and generate a quasibound state. To obtain real binding, assistance from the $I_{KN} = 1$ S-wave state and the NN P-wave attraction is necessary. Thus, the NN interactions repulsive at large distances in the $I_{NN} = 0$, $S_{NN} = 0$, $L_{NN} = 1$ waves do not support bound states. However, such states may be generated by $I_{NN} = 1$, $S_{NN} = 1$, $L_{NN} = 1$ interactions. Here, the analysis becomes more subtle as the NN interaction is strongly spin dependent. The energy given in Table V corresponds to $J = 2$ ($^3P_2$) wave in the NN subsystem where

TABLE V. The binding energy and width (in MeV) of the $\bar{K}NN$ $I_{\rm tot} = 3/2$, $I_{NN} = 1$ space-asymmetric states. In the NN subsystem $^{2S+1}L_J = {}^3P_2$. The last column gives the radius mean squared of the NN separation (in fm).

	I_{NNK}	I_{NN}	E_B (MeV)	Γ (MeV)	$R_{\rm rms}$ (fm)
K^-nn	3/2	1	48.5	36	4.9

TABLE VI. Binding energies and widths (in MeV) of the $I_{\rm tot} = 0$, $\bar{K}NNN$, space-symmetric states obtained with the two-channel $\bar{K}N$, $\Sigma\pi$-channel multiple-scattering formulation. The results on the left are based on the KWW [10] parameters. The results on the right are calculated with modified KWW* parameters that set the $\Lambda(1405)$ set to 1405 MeV. The first column specifies meson-nucleon partial waves involved. The widths do not describe nonmesic capture modes.

	E_B	Γ	E_B	Γ
S	103	29	142	25
$S + P$	119	23	153	21

the interaction is the most attractive. This $\bar{K}NN$ system is large and loosely bound, by about 1.5 MeV in the $\Sigma(1385)N$ configuration. In this calculation the S-wave parameters come from AM [20] and the calculated energy is uncertain, as the involved K^-n parameters are poorly known. The experimental detection would be very difficult, nevertheless, a more precise analysis of the spin and isospin structure of such states is of interest in the context of K^-D atoms and will be performed elsewhere.

B. $\bar{K}NNN$ and $\bar{K}NNNN$ systems

The discussion of these systems is limited to the states of the simplest symmetry. The fixed nucleon model generates a contracting potential that in $\bar{K}NNN$ systems may be, to a good approximation, presented in the form

$$E^c(R_x, R_y, R_z) = -V_{NNN}\{1 - C\exp[-\lambda_s(R_x + R_y + R_z)]\}[\exp(-\lambda_l R_x) + \exp(-\lambda_l + R_y) + \exp(-\lambda_l R_z)] - V(\infty), \quad (71)$$

where R_x, R_y, R_z are the internucleon distances. The short range behavior at the triple coincidence may be obtained analytically and $C = 0.42$, other parameters being numerical.

With the $\bar{K}N$ parameters of Refs. [10,20] and $I_{\rm tot} = 0$ the parameters are obtained in the range $V_{NNN} \sim 150$–200 MeV, $\lambda_s \simeq 4.5$ fm, $\lambda_l \sim 1.8$–1.9 fm. For $I_{\rm tot} = 1$ one has $V_{NNN} \sim 50$–60. $V(\infty)$ is the binding of $\bar{K}N$ into $\Lambda(1405)$ in the S-wave case or $\Sigma(1385)$ in the $S + P$-wave case. For $I_{\rm tot} = 0$ the corresponding binding energies are given on the left side of Table VI. These numbers may be compared to the simplest version of this model—the S-wave interactions described by the single $\bar{K}N$ channel—which produce 91-MeV binding.

The modified version of the KWW model with parameters from Table I fixed to set the $\Lambda(1405)$ energy to 1405 MeV yields much stronger contracting forces, $V_{NNN} \sim 250$–350 MeV and $\lambda_l \sim 2.1$–2.3 fm. The states indicated on the right side in Table VI are bound very deeply. The basic NNN systems obtained with our variational wave function are overbound by about 2 MeV and this value has already been subtracted from the numerical $\bar{K}NNN$ energies.

There may exist a number of states in the $\bar{K}NNNN$ systems. In Tables VI–VIII one finds only the states with the simplest symmetry, which involve wave functions symmetric under exchange of the nucleon coordinates. In the absence of

TABLE VII. Binding energies and widths (in MeV) of the $I_{\rm tot} = 1$, $\bar{K}NNN$, space-symmetric states obtained with the two-channel $\bar{K}N$, $\Sigma\pi$-channel multiple-scattering formulation. These states are formed as a result of the P-wave interactions with some assistance of the S-wave attraction.

	E_B	Γ
$S+P$	63	38

the $\bar{K}$ meson the basic α particle structure is used and only the S-wave NN interactions are included. With the tensor interactions described by Eq. (27) this α system is overbound by about 10 MeV, and this value has been subtracted from the calculated $\bar{K}NNNN$ levels.

C. Level widths

Level widths are calculated as twice the expectation value of $\mathrm{Im}V_K$. The $\bar{K}N$ resonant lifetimes are strongly energy dependent, being very short at the resonance, becoming longer below the resonant energies, and staying infinite below the thresholds of the decay channels. This trend is reflected by $\mathrm{Im}V_K$ in Fig. 1. The energy dependence contained in the amplitude $f_{KN}(-E_B - E_{\rm recoil})$ of Eq. (1) is traded into the space dependence $f_{KN}(V_K)$. These two types of averaging give fairly close results provided the final binding energy is located well above the threshold of the decay channels. Let us indicate some consequences of this relation.

The states generated by the P-wave interactions given in Tables IV, V, and VII correspond to a fairly loosely bound $\Sigma(1385)$ and the widths of quasibound states are essentially equal to the width of the $\Sigma(1385)$. This comes as a result of the peripheral binding and weak effects of the collision broadening in the P-wave resonances. In these states, the V_K underestimates slightly the average $-E_B - E_{\rm recoil}$ and the real widths might be smaller. For the binding energies in the range 60–90 MeV the V_K is too small at large distances and too large at small distances with a reasonably good average. Let us notice that the level widths generated by the $S+P$ interactions are smaller than those generated by the S waves alone. This is due to three factors: the width of $\Lambda(1405)$ is larger than the width of $\Sigma(1385)$, the collision broadening in P waves is small and the systems due to the $S+P$ interactions are less compressed. Let us also notice very strong sensitivity to the input $\bar{K}N$ amplitudes. The few examples of $\mathrm{Im}F_{100}$ given in Table I and the differences of the widths in the $I_{\rm tot} = 1/2$, $I_{NN} = 0$, $\bar{K}NN$ state visualize this point.

TABLE VIII. Binding energies and widths (in MeV) of the $\bar{K}NNNN$, space-symmetric, $S_{\rm tot} = 0$, $I_{\rm tot} = 1/2$ states. See captions to Table VI.

	E_B	Γ	E_B	Γ
S	121	25	170	10
$S+P$	136	20	172	10

In cases of very large binding, in the range of 120–200 MeV, one $(\Sigma\pi)$ or two $(\Sigma\pi, \Lambda\pi)$ decay channels are blocked and the widths calculated here are overestimated. Such a situation is likely to happen in the $\bar{K}\alpha$ state. To account for that effect, the calculation of the contracting potential was repeated in an optical potential manner. So, the momenta in the decay channels $\Sigma\pi$, $\Lambda\pi$ were related to the binding energy E_B and allowed no outgoing waves. Such a calculation results in a stronger binding. In the KWW* model one obtains binding of 220 instead of the 170 given in Table VIII. The real decay width is now given by the multinucleon capture mode.

The multinucleon captures are initiated by the nonmesic $\bar{K}NN \to YN$ mode and the branching ratio for this process is known from emulsion studies to be about 20% in light nuclei [35]. The emulsion data are obtained with stopped $\bar{K}$ mesons and pertain to the nuclear surfaces. An extrapolation in terms of a characteristic nuclear densities ρ and two-body phase-space L

$$\Gamma_{\rm multi} \simeq L\varrho^2\gamma \tag{72}$$

for this decay was attempted in Ref. [4]. A constant γ may be fixed to the emulsion branching ratio and a 20-MeV level width in the nuclear matter at 90-MeV binding was obtained. In the strongly bound, few-body systems the kinematics of the decay is different because the residual nucleons also take sizable recoil energies. Roughly, for a three body decay $L \sim Q^2$ where Q is the decay energy. Again, an extrapolation from the emulsion data in terms of the available phase space and the involved nuclear density yields nonmesic capture widths in $\bar{K}\alpha$ in the 10- to 30-MeV range. These estimates are some what larger than the 12 MeV obtained for the $\bar{K}NNN$ system in Ref. [9]. Unfortunately such extrapolations are uncertain as the energy dependence in γ might be large and the Q value is not known. Help from new experiments is necessary to settle these questions.

VI. CONCLUSIONS

In this article a new method to calculate the deeply bound $\bar{K}NN$, $\bar{K}NNN$, and $\bar{K}NNNN$ states has been presented. The calculation consists of two steps. First a wave function involving strongly correlated $\bar{K}N$ subsystems is found in a fixed nucleon approximation. This step also allows one to find potentials due to the $\bar{K}$ meson that tend to contract the internucleon distances. Next, these correlated wave functions and contracting potentials are used as input in the Schrödinger or variational calculations for the $\bar{K}$-few-nucleon binding.

The lowest binding energies based on a phenomenological $\bar{K}N$ input fall into the 40- to 80-MeV range for $\bar{K}NN$, 90–150 MeV for $\bar{K}NNN$, and 120–220 MeV for $\bar{K}\alpha$ systems. The uncertainties are due to unknown $\bar{K}N$ interactions in the distant subthreshold energy region.

We obtain at least partial answers to the basic questions presented in the introduction.

(i) The binding mechanism: the dominant mechanism of the attraction is related to the $\Lambda(1405)$ state. This fact

has been known for a long time. In addition, it is found here, that the $\Sigma(1385)$ contributes significantly to the structure of the $\bar{K}$-few-N bound states but much less to the actual binding energies. The bound states are built from the strongly correlated $\bar{K}N$ subsystems. At central densities these correlations resemble the $\Lambda(1405)$ and at peripheries the correlations are made by the quasifree $\Sigma(1385)$. Sizable fractions of the binding energies are contained in the $\bar{K}N$ correlations. One consequence is that even with the strong bindings the nucleon densities are not dramatically enhanced as in Ref. [9] but can become a factor 2–4 larger than the standard nuclear matter density ρ_o.

The presence of $\Sigma(1385)$ resonances in the few-nucleon systems generates new states. These are predominantly P-wave states or states built on the P-wave NN interactions and are usually broad and loosely bound developing long tails built from the $\Sigma(1385)$ correlation.

(ii) The control of technical questions: the choice of correlated wave functions removes the difficulties related to the uncertain $\bar{K}N$ interaction range and allows one to use realistic NN interactions. The recoil energy of the $\bar{K}N$ subsystems with respect to the residual nucleons is described only in an average sense. This seems to be the weakest part of this method.

(iii) The widths are related to the lifetimes of the $\Lambda(1405)$ and $\Sigma(1385)$ enhanced by the collision broadenings. Under the phenomenological $\bar{K}N$ interactions (the Λ pole located at 1412–17i MeV) the $\bar{K}$-few-N states are $\sim$40 MeV wide.

However, the models with the Λ pole located at $\sim 1405 - 25i$ MeV generate $\bar{K}$-few-N states that are more deeply bound. These may be either very broad or quite narrow. With the binding energies in the 60–80 MeV range (the $\bar{K}NN$ case) very broad—up to 90 MeV—states are obtained. However, with the bindings of 120 MeV ($\bar{K}NNN$) or 170 MeV ($\bar{K}NNNN$) the single-nucleon decay modes are effectively blocked. The widths are strongly reduced and the main decay modes are due to multinucleon $\bar{K}$ captures. These widths are hard to predict, a simple model suggested here generate widths of about 20 MeV.

A simple physical picture emerges from this approach. The mesons are strongly correlated to slowly moving nucleons. The correlations are of the $\Lambda(1405)$ type at large densities and of the $\Sigma(1385)$ type in the peripheries. Each $\bar{K}N$ pair has a good chance to stay also in the $\Sigma\pi$ form. The structure is rather loose as sizable fractions of the binding energies are hidden in the short-ranged correlations.

ACKNOWLEDGMENTS

This work is supported by the KBN Grant 1P0 3B 04229 and the EU Contract No. MRTN-CT-2006-035482, "FLAVIAnet." Part of this work was carried out while one of the authors (S.W.) was at the Helsinki Institute of Physics.

APPENDIX A: PROPAGATORS

Several formulas for kernels of multiple-scattering equations are collected in this appendix.

For Yamaguchi form factors, the propagators $G_{i,j}$ yield analytic expressions. Thus for two consecutive S-wave interactions one has

$$G(r,k)^{ss} = \frac{1}{4\pi r} v(k)^2 \Big[\exp(ikr) - \exp(\kappa r) - r\frac{\kappa^2 + k^2}{2\kappa} \exp(-\kappa r) \Big], \tag{A1}$$

where $\mathbf{r} = \mathbf{x}_i - \mathbf{x}_j$ and the indices i, j referring to the nucleon sites are suppressed. For an initial S-wave scattering followed by a P-wave scattering G becomes a vector

$$\mathbf{G}(r,k)^{\mathrm{sp}} = \mathbf{r} G^{\mathrm{sp}}(r,k), \tag{A2}$$

$$G^{\mathrm{sp}} = \frac{1}{4\pi r} v(k)^2 \Big\{ \exp(ikr)(ikr - 1) - \exp(\kappa r) \times \Big[1 + \kappa r + \frac{r^2(\kappa^2 + k^2)}{2} + \frac{r^3(\kappa^2 + k^2)^2}{8\kappa} \Big] \Big\}. \tag{A3}$$

For two consecutive P-wave interactions the propagator is a tensor of the form

$$\mathbf{G}(r,k)^{pp}|_{nm} = v(k)^2 \big(\delta_{nm} G_O^{pp} + r_n r_m G_T^{pp} \big). \tag{A4}$$

These functions may be expressed in terms of basic integrals

$$g_n(r) = \frac{4\pi}{(2\pi)^3} \int d\mathbf{p} \exp(ikr) \Big(\frac{\kappa^2}{\kappa^2 + p^2} \Big)^n \frac{1}{p^2 - k^2}, \tag{A5}$$

which give by recurrence

$$g_1(r) = \frac{\exp(ikr) - \exp(\kappa r)}{r}, \tag{A6}$$

$$g_2(r) = g_1(r) - \frac{\kappa^2 + k^2}{2\kappa} \exp(-\kappa r)$$

$$g_3(r) = g_2(r) - \frac{(\kappa^2 + k^2)^2}{8\kappa^3} (1 + \kappa r) \exp(-\kappa r), \tag{A7}$$

$$g_4(r) = g_3(r) - \frac{(\kappa^2 + k^2)^3}{16\kappa^5} \Big[1 + \kappa r + \frac{(\kappa r)^2}{3} \Big] \exp(-\kappa r)$$

and finally

$$G_O^{pp} = \frac{g_4(r)'}{r}, G_T^{pp} = \frac{g_4(r)''}{r^2} - \frac{g_4(r)'}{r^3}. \tag{A8}$$

APPENDIX B: ISOSPIN SYMMETRY

It is assumed here that the isospin is conserved in the quasibound states of $\bar{K}$ mesons. In the lowest S-wave states of the $\bar{K}NN$ systems the isospin wave functions may be built on isosinglet or isotriplet NN states. From the experimental point of view, the most interesting one seems to be

$$\Psi_1^{1/2} = \{\{NN\}^1 K\}^{1/2} = \sqrt{3}/2 \{\{NK\}^0 N\}^{1/2} + 1/2 \{\{NK\}^1 N\}^{1/2}, \tag{B1}$$

where in $\Psi_1^{1/2}$ the upper index denotes isospin $I_{\rm nucl}$ and the lower index denotes the spin of the two nucleons. On the right side the isospin content in the $\bar{K}N$ subsystem is given. This state is a mixture of K^-pp and $\bar{K}^0np$ and is frequently named K^-pp because it can be experimentally accessed via this entrance channel. The NN spin in this state is $S=0$ and the effective $\bar{K}N$ interaction amplitude obtained from Eq. (B1) becomes

$$f_{KN} = 3/4 f^0_{KN} + 1/4 f^1_{KN}. \tag{B2}$$

Another $\bar{K}NN$ state of interest is built on the NN isosinglet

$$\Psi_0^{1/2} = \{\{NN\}^0 K\}^{1/2} = -1/2\{\{NK\}^0 N\}^{1/2} + \sqrt{3}/2\{\{NK\}^1 N\}^{1/2}. \tag{B3}$$

This state is a mixture of K^-np and $\bar{K}^0nn$ that might be reached by the K^-np entrance channel. Now the NN spin is $S=1$ and the effective $\bar{K}N$ interaction amplitude obtained from Eq. (B3) becomes

$$f_{KN} = 1/4 f^0_{KN} + 3/4 f^1_{KN}. \tag{B4}$$

The S-wave $\bar{K}N$ interaction in the $\Psi_0^{1/2}$ state is much less attractive than in the $\Psi_1^{1/2}$ state since the $\Lambda(1405)$ contribution is reduced. However, this is offset by the strong short-range attraction in the NN system due to the tensor force. An additional attractive force is due to a larger contribution from the $\Sigma(1385)$ resonance.

Finally one may have total isospin 3/2 states of the type K^-nn or $\bar{K}^0pp$

$$\Psi_1^{3/2} = \{\{NN\}^1 K\}^{3/2} = \{\{NK\}^1 N\}^{3/2}. \tag{B5}$$

Those states, involve weakly attractive and uncertain, S-wave $\bar{K}N$ $I=1$ amplitudes. A deeper state can in principle be built on the stronger P-wave interactions. Its existence and the chances for detection present a situation that is more difficult than the other cases.

For the three-nucleon problem we retain the dominant structure of the triton and helium isospin symmetry. The $\bar{K}NNN$ wave function is assumed to be of the form

$$\Psi^T = \frac{1}{\sqrt{2}}\{\{\{NN\}^{0,1}N\}^{1/2} + \{\{NN\}^{1,0}N\}^{1/2}\}K\}^T, \tag{B6}$$

where the pair of indices denote spin and isospin of the NN pair.

Recoupling to the $\bar{K}N$ system leads in the total $T=0$ state to the relation

$$\Psi^0 = \sqrt{1/2}\{\{NN\}^1\{NK\}^1 + \{NN\}^0\{NK\}^0\}^0 \tag{B7}$$

TABLE IX. Isospin composition of antikaon nucleon scattering amplitudes. $I_{\rm tot}$ = total isospin, $I_{\rm nucl}$ = isospin of nucleons, f_i = $\bar{K}N$ amplitudes of isospin, i.

System	$I_{\rm tot}$	$I_{\rm nucl}$	f_{KN}
$\bar{K}NN$	$\frac{3}{2}$	1	f_1
$\bar{K}NN$	$\frac{1}{2}$	1	$\frac{3}{4}f_0 + \frac{1}{4}f_1$
$\bar{K}NN$	$\frac{1}{2}$	0	$\frac{1}{4}f_0 + \frac{3}{4}f_1$
$\bar{K}NNN$	0	$\frac{1}{2}$	$\frac{1}{2}f_0 + \frac{1}{2}f_1$
$\bar{K}NNN$	1	$\frac{1}{2}$	$\frac{1}{6}f_0 + \frac{5}{6}f_1$
$\bar{K}NNNN$	$\frac{1}{2}$	0	$\frac{1}{3}f_0 + \frac{2}{3}f_1$

and in this case the $\bar{K}N$ interaction amplitude is

$$f^s = 1/2 f^0_{KN} + 1/2 f^1_{KN}. \tag{B8}$$

Likewise for the total isospin 1 system

$$f^s = 1/6 f^0_{KN} + 5/6 f^1_{KN}. \tag{B9}$$

These amplitudes are collected into Table IX.

APPENDIX C: THREE NUCLEONS, *S*-WAVE INTERACTIONS

The energy eigenvalue is obtained by the simultaneous solution of three equations

$$\psi^s_1 + G^{ss}_{1,2} f^s \psi_2 + G^{ss}_{1,3} f^s \psi^s_3 = 0 \tag{C1}$$

$$\psi^s_2 + G^{ss}_{2,3} f^s \psi^s_3 + G^{ss}_{2,1} f^s \psi^s_1 = 0 \tag{C2}$$

$$\psi^s_3 + G^{ss}_{3,1} f^s \psi^s_1 + G^{ss}_{3,2} f^s \psi^s_2 = 0, \tag{C3}$$

which require the eigenvalue condition

$$D_{3s} \equiv 1 - (f^s)^2\left(G^{ss}_{1,2}G^{ss}_{1,2} + G^{ss}_{1,3}G^{ss}_{1,3} + G^{ss}_{3,2}G^{ss}_{3,2}\right) + 2(f^s)^3 G^{ss}_{1,2}G^{ss}_{2,3}G^{ss}_{3,1} = 0. \tag{C4}$$

This equation is to be solved numerically. A helpful guide to find the symmetry of two physically meaningful solutions is the situation of two equal NN separations $r_{12} = r_{13}$. Dropping the upper indices one obtains the factorized form

$$D_{3s} = (1 - f G_{1,2})(1 + f G_{1,2} - 2 f^2 G^2_{1,3}). \tag{C5}$$

The first factor corresponds to an antisymmetric solution with the meson sticking to two nucleons only. The second factor generates a solution symmetric with the interchange of nucleons 1 and 2. These solutions are a direct continuation of the two solutions obtained in the $\bar{K}NN$ systems.

[1] T. Suzuki *et al.*, Phys. Lett. **B597**, 263 (2004).
[2] M. Iwasaki, *Conference on Exotic Atoms*, Austrian Academy of Science Press (2005), p. 63.
[3] M. Agnello (FINUDA Collaboration), Phys. Rev. Lett. **94**, 212303 (2005).
[4] S. Wycech, Nucl. Phys. **A450**, 399c (1986).
[5] E. Friedman and A. Gal, Phys. Rep. **452**, 89 (2007).
[6] E. Oset and H. Toki, Phys. Rev. C **74**, 015207 (2006).
[7] V. K. Magas, E. Oset, A. Ramos, and H. Toki, Phys. Rev. C **74**, 025206 (2006).
[8] Y. Akaishi and T. Yamazaki, Nucl. Phys. **A792**, 229 (2007).
[9] Y. Akaishi and T. Yamazaki, Phys. Rev. C **65**, 044005 (2002).
[10] W. Krzyzanowski, J. Wrzecionko, and S. Wycech , Acta Phys. Pol. B **6**, 259 (1975).
[11] W. Weise, *Conference on Exotic Atoms*, Austrian Academy of Science Press (2005), p. 35.

[12] A. Dote and W. Weise, Prog. Theor. Phys. Suppl. **168**, 593 (2007).
[13] N. V. Shevchenko, A. Gal, J. Mareš, and J. Révai, Phys. Rev. C **76**, 044004 (2007).
[14] N. V. Shevchenko, A. Gal, and J. Mareš, Phys. Rev. Lett. **98**, 082301 (2007).
[15] Y. Ikeda and T. Sato, Phys. Rev. C **76**, 035203 (2007).
[16] S. Wycech and A. M. Green, Int. J. Mod. Phys. A **22**, 629 (2007).
[17] R. B. Wiringa, V. G. J. Stoks, and R. Schiavilla, Phys. Rev. C **51**, 38 (1995).
[18] K. A. Brueckner, Phys. Rev. **89**, 834 (1953).
[19] L. L. Foldy and J. D. Walecka, Ann. Phys. (NY) **54**, 447 (1969).
[20] A. D. Martin, Nucl. Phys. **B179**, 33 (1981).
[21] B. R. Martin and M. Sakitt, Phys. Rev. **183**, 1345 (1969) ; Phys. Rev. **183**, 1352 (1969) .
[22] R. Staronski and S. Wycech, J. Phys. G **13**, 1361 (1987).
[23] R. H. Dalitz and A. Deloff, J. Phys. G **17**, 289 (1991).
[24] M. Alberg, E. M. Henley, and L. Wilets, Ann. Phys. (NY) **96**, 43 (1976).
[25] J. Wrzecionko and S. Wycech, Czech. J. Phys. B **24**, 1293 (1974).
[26] M. Iwasaki *et al*., Phys. Rev. Lett. **78**, 3067 (1997).
[27] G. Beer *et al*., Phys. Rev. Lett **94**, 212302 (1997).
[28] T. Hyodo and W. Weise, Phys. Rev. C **77**, 035204 (2008).
[29] E. Oset, A. Ramos, and C. Bennhold, Phys. Lett. **B527**, 99 (2002).
[30] B. Borasoy, U.-G. Meißner, and R. Nißler, Phys. Rev. C **74**, 055201 (2006).
[31] Particle Data Group, J. Phys. G **33**, 1027 (2006).
[32] O. Braun *et al*., Nucl. Phys. **B129**, 1 (1979).
[33] W. Cameron *et al*., Nucl. Phys. **B143**, 189 (1978).
[34] T. Yamazaki and Y. Akaishi, Phys. Rev. C **76**, 045201 (2007).
[35] R. Roosen *et al*., Nuovo Cimento A **49**, 217 (1979).